© 2015. Published by The Company of Biologists Ltd | The Journal of Experimental Biology (2015) 218, 991-998 doi:10.1242/jeb.117101

RESEARCH ARTICLE

Functional morphology of the *Alligator mississippiensis* larynx with implications for vocal production

Tobias Riede[1,*], Zhiheng Li[2], Isao T. Tokuda[3] and Colleen G. Farmer[4]

ABSTRACT

Sauropsid vocalization is mediated by the syrinx in birds and the larynx in extant reptiles; but whereas avian vocal production has received much attention, the vocal mechanism of basal reptilians is poorly understood. The American alligator (*Alligator mississippiensis*) displays a large vocal repertoire during mating and in parent–offspring interactions. Although vocal outputs of these behaviors have received some attention, the underlying mechanism of sound production remains speculative. Here, we investigate the laryngeal anatomy of juvenile and adult animals by macroscopic and histological methods. Observations of the cartilaginous framework and associated muscles largely corroborate earlier findings, but one muscle, the cricoarytenoideus, exhibits a heretofore unknown extrinsic insertion that has important implications for effective regulation of vocal fold length and tension. Histological investigation of the larynx revealed a layered vocal fold morphology. The thick lamina propria consists of non-homogenous extracellular matrix containing collagen fibers that are tightly packed below the epithelium but loosely organized deep inside the vocal fold. We found few elastic fibers but comparatively high proportions of hyaluronan. Similar organizational complexity is also seen in mammalian vocal folds and the labia of the avian syrinx: convergent morphologies that suggest analogous mechanisms for sound production. In tensile tests, alligator vocal folds demonstrated a linear stress–strain behavior in the low strain region and nonlinear stress responses at strains larger than 15%, which is similar to mammalian vocal fold tissue. We have integrated morphological and physiological data in a two-mass vocal fold model, providing a systematic description of the possible acoustic space that could be available to an alligator larynx. Mapping actual call production onto possible acoustic space validates the model's predictions.

KEY WORDS: Larynx, Syrinx, Vocal production, Vocal control, Sauropsida, Extracellular matrix, Hyaluronan

INTRODUCTION

Crocodilian vocal repertoires consist of a diverse array of sound types (Herzog and Burghardt, 1977; Campbell, 1973; Garrick and Lang, 1977; Watanabe, 1980; Hunt and Watanabe, 1982; Vliet, 1989; Britton, 2001; Vergne et al., 2009; Wang et al., 2007; Todd, 2007; Wang et al., 2009; Sicuro et al., 2013) but little is known about how such variability is generated. Here, we focus on the morphology and performance of the structures that determine fundamental frequency (F_0) – a critical acoustic parameter that can reveal relevant information about the sender, and is therefore a prime selective target. To date, our understanding of the underlying mechanism of F_0 control in sauropsids is primarily limited to birds (Riede and Goller, 2010; Goller and Riede, 2013), whose syrinx-driven vocalization differs significantly from that of basal sauropsids. The American alligator is an ideal model system for elucidating the mechanism of vocal production in basal saurposids. It has a diverse vocal repertoire that, like mammals, is generated by the larynx. In mammals, laryngeal sound production results both from active control of laryngeal movement and breathing and the passive mechanical properties of vocal folds. Before voice onset, active positioning of the vocal folds close to the midline narrows the space between the folds (i.e. the glottis), thereby increasing the resistance and the magnitude of the transglottal pressure gradient. This produces a high-speed intra-glottal airflow with associated pressure changes on the vocal fold surfaces that, in turn, facilitate self-sustaining tissue oscillations (Titze, 1988). This was first demonstrated by blowing air through an excised alligator larynx (Müller, 1839) and confirmed by subglottal pressure and airflow measurements made in spontaneously calling animals (Riede et al., 2011). The rate of these oscillations depends on lung pressure (affecting transglottal pressure gradient), vocal fold geometry (length, thickness and depth), and vocal fold tension (similar to string oscillations in a string instrument). The vocal fold vibrations are induced by airflow and are self-sustained.

Alligators produce sounds with an F_0 between ~50 and 1200 Hz. Lung pressure ranges between 0.5 and 6 kPa during vocalization (Riede et al., 2011). Vocal fold length scales isometrically with body mass (Riede et al., 2011), but actual mechanical properties of the vocal folds were unknown. To investigate mechanical properties, we used tensile tests to measure elasticity and stress relaxation. Because tissue mechanical properties depend on both the composition and organization of fibrillar proteins (i.e. collagen and elastin) and the content and distribution of amorphic substances (i.e. hyaluronan), we used several histological staining techniques and computer tomographic imaging to refine our understanding of the alligator's laryngeal morphology. Finally, a computer simulation of the alligator's larynx was used to integrate morphological and physiological data to explore boundaries of the alligator's available acoustic space.

RESULTS

Skeletal framework of the larynx

The larynx consists of three cartilages (Fig. 1 and supplementary material Fig. S1). The cricoid cartilage forms a complete ring at the cranial end of the trachea. The arytenoid cartilages are two symmetric arches positioned rostrally from the cricoid ring. They are attached to the cricoid via one dorsal and one ventral joint. Each arch consists of a dorsal and a ventral branch. The basihyoid is an enlarged, cup-like structure housing all laryngeal elements.

[1]Department of Physiology, Midwestern University, Glendale, AZ 85308, USA. [2]Department of Geological Sciences, University of Texas at Austin, Austin, TX 78712, USA. [3]Department of Mechanical Engineering, Ritsumeikan University, Shiga, 525-8577, Japan. [4]Department of Biology, University of Utah, Salt Lake City, UT 84112, USA.

*Author for correspondence (triede@midwestern.edu)

Received 25 November 2014; Accepted 24 January 2015

The Journal of Experimental Biology (2015) 218, 991-998 doi:10.1242/jeb.117101

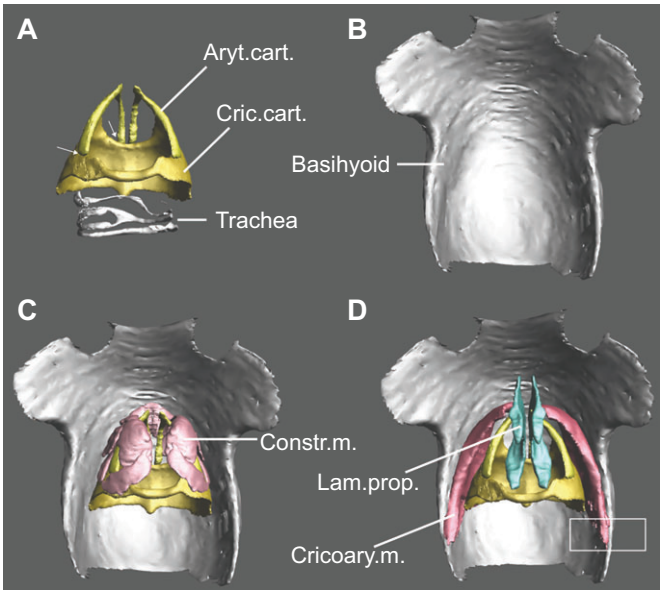

Fig. 1. Alligator cartilagenous larynx in dorsal view. (A) The larynx consists of the cricoid cartilage and two arches of arytenoid cartilages. Each arytenoid consists of a dorsal branch and a ventral branch. Two arrows indicate flexible joint-like connections between left arytenoid and cricoid cartilage. The larynx sits inside a cup-like basihyoid cartilage (B). Two sets of laryngeal muscles exist in the alligator larynx. (C) The constrictor laryngeus muscle (constr.m.) causes adduction. (D) The cricoarytenoid muscle (cricoary.m.) would cause abduction. Its attachment to the medial side of the caudal basihyoid would most likely facilitate a change in vocal fold length. The white rectangle indicates the location of the higher magnification images in Fig. 4.

Epithelium and connective tissue in vocal folds

The vocal fold epithelium consists of cuboid ciliated cells covering a thick layer of extracellular matrix (ECM) and muscles (Fig. 2A). Serous epithelial cells limited to the pharyngeal side of the vocal folds (Fig. 2B) remained intensely positively stained after hyaluronidase treatment and contain a range of different glucoseaminoglycans. The Alcian Blue stain before (Fig. 2C) and after (Fig. 2D) removal of hyaluronan by hyaluronidase digestion indicates that much of the positive staining in the vocal fold can be attributed to hyaluronan.

The ECM is also rich in collagen fibers, and the area between the epithelium and the center of the vocal fold exhibits a gradient of decreasing collagen content. A dense layer of collagen below the epithelium (Fig. 2E,F) contained fibers oriented parallel to the epithelial surface with an average thickness of 2.4 µm (2.4±0.8 µm; mean±s.d.; measured in three juvenile alligators). In the center of the vocal fold, collagen fibers were less densely packed, had smaller average diameters (0.9±0.7 µm; mean±s.d.), and were oriented randomly.

Laryngeal muscles

The *musculus cricoarytenoideus* originates laterally on the cricoid cartilage (Fig. 3). It extends to the rostro-lateral aspect of the dorsal branch of the arytenoid and into the soft connective tissue of the vocal folds (Fig. 3, L2). Contraction of this cranial aspect of the muscle would pull on the rostral end of the arytenoid arch, causing movement laterad and opening the glottis (vocal fold abduction). There is also a caudal branch of the muscle attaching to the cricoid and to the medial side of the basihyoid (Fig. 4). This newly described attachment to the basihyoid confers this muscle's extrinsic properties. An isolated contraction of the caudal portion would pull the entire larynx caudally, exerting a strain on the vocal folds along their longitudinal (rostro-caudal) axis. This would generate tensile stress, a mechanism most important in facilitating variation in F_0, but previously thought to be absent in alligators (Riede et al., 2011).

The glottal adductor (musculus constrictor laryngis, Söller, 1931) consists of two branches, a pars ventralis and pars dorsalis. The left and right branches of the pars dorsalis meet in a raphe on the dorsal

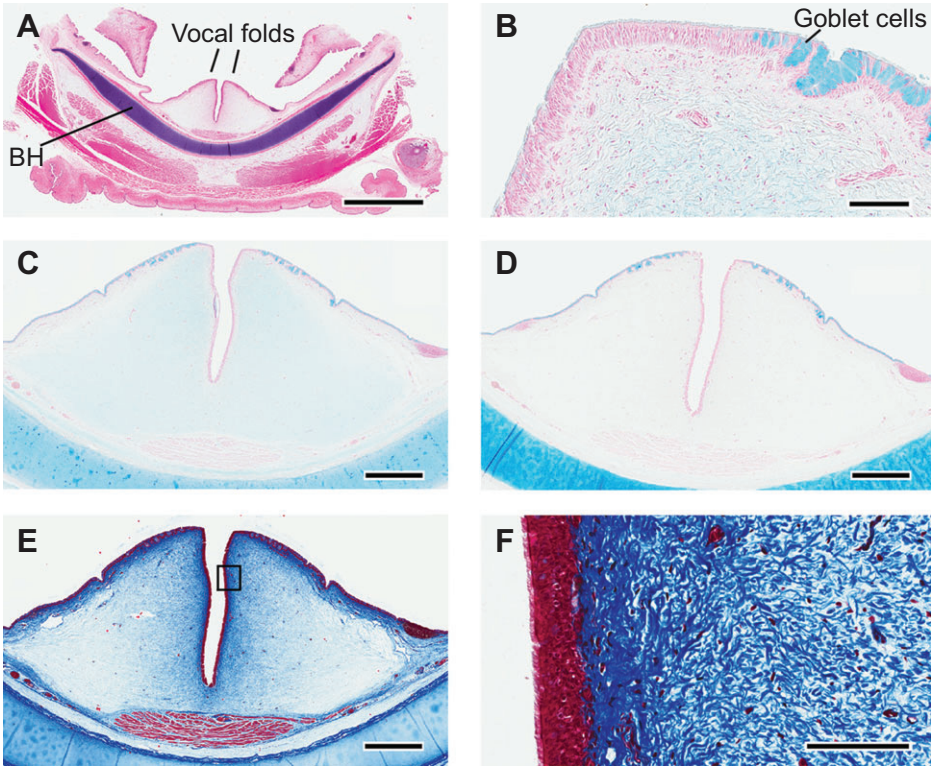

Fig. 2. Cross-sections of an alligator larynx. Images from a single male of 590 g body weight. The section level was rostral from the arytenoid cartilages. (A) H&E stain providing an overview of the vocal folds (BH, basihyoid). (B) Alcian Blue stain. (C) Alcian Blue stain of both vocal folds. The light blue stain indicates presence of glucoseaminoglycans. (D) Alcian Blue stain of vocal folds after hyaluronidase incubation. The light blue stain of the vocal fold as in C is not visible, but note that serous cells in epithelium are still firmly blue. This suggests that hyaluronan was the predominant component of the glucoseaminoglycans in the extracellular matrix of the vocal folds. (E) Masson's trichrome stain of both vocal folds. The intraglottal and pharyngeal superficial area of the extracellular matrix shows high concentrations of collagen. The blue stain indicates collagen fibers. (F) Higher magnification of the area indicated by a rectangle in E. Collagen fibers are primarily parallel to the cutting surface below the epithelium but more loosely and randomly oriented in deeper layers. Scale bars: 5 mm (A); 100 µm (B,F); 1 mm (C–E).

The Journal of Experimental Biology

The Journal of Experimental Biology (2015) 218, 991-998 doi:10.1242/jeb.117101

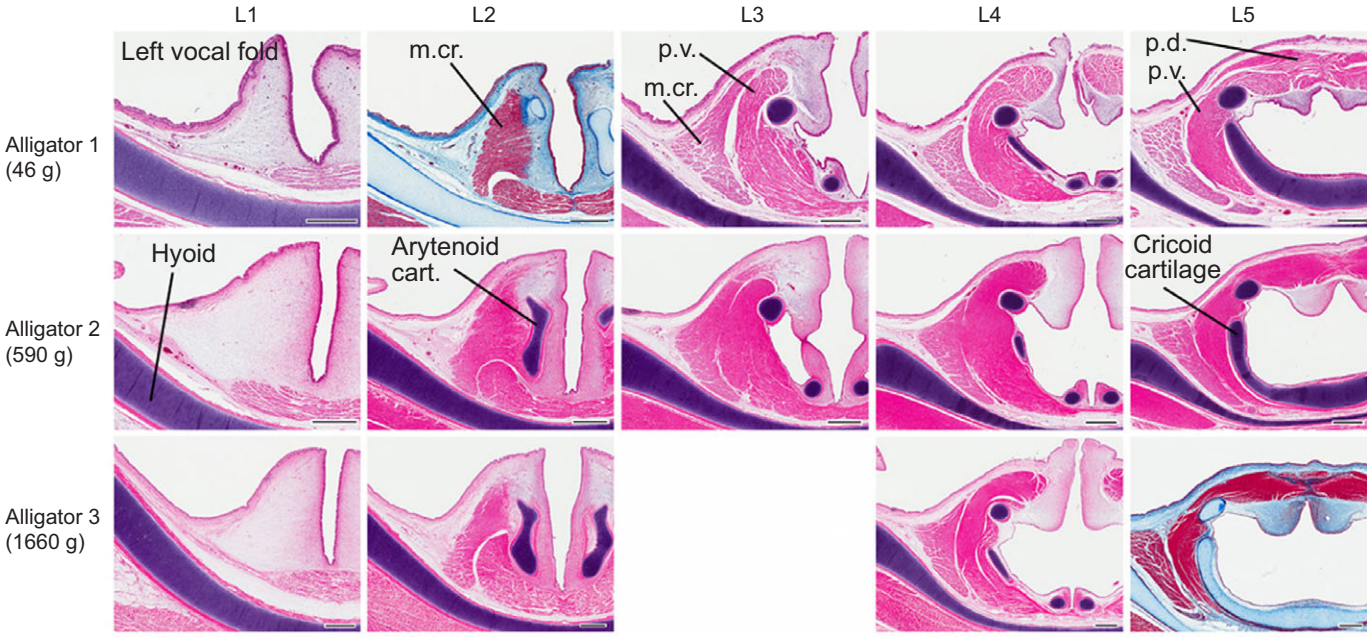

Fig. 3. Serial cross-sections of three alligator larynges from rostral (L1) to caudal (L5). Masson's Trichrome stain for L2, alligator 1 and for L5, alligator 3. H&E stains in all other sections. m.cr., musculus cricoarytenoideus; p.d., pars dorsalis of constrictor laryngis muscle; p.v., pars ventralis of constrictor laryngis muscle. Scale bars: 500 μm (alligator 1); 1 mm (alligators 2 and 3).

midline rostral to the cricoid. The muscle attaches laterally to the dorsal branch of the arytenoid (Fig. 3, L5). Contraction of the dorsal portion would adduct the dorsal aspects of the vocal folds. The pars ventralis runs between the cranial end of the dorsal arytenoid arch and a ventral raphe, where the left and right portions of this muscle are inserted. A contraction of the pars ventralis would adduct the ventral aspects of the vocal folds and reduce the size of the lateral ventricle (Fig. 3). Because the dorsal portion is postioned caudal and the ventral portion rostral, differential contraction of both portions is expected to cause differential tension in the dorso-ventral axis of the vocal fold.

Tensile tests

Tensile tests were performed on the lamina propria of the vocal folds to determine elasticity and stress relaxation behavior. The tissue showed a linear stress–strain response in the low-strain region and a nonlinear relationship in the high-strain region during a cyclic loading–unloading test (Fig. 5A). Linear and nonlinear models (Table 1) reached regression coefficients of 0.97 and higher. Tissue stress ranged from 1 to 600 kPa for a vocal fold length of 1 cm at strains of up to 35%. F_0 values fell between 50 and ~1200 Hz (Fig. 5B) at the same strain values, and correspond well with reported ranges in F_0 for natural calls of juvenile animals (e.g. Britton, 2001; Vergne et al., 2009). Hysteresis ranged from 31 to 55%. Stress relaxation ranged from 18 to 44%, and peak stress was reduced by 50% within the initial 205 to 315 ms ('stress half life') (Table 1). This initial stress relaxation likely has a large influence on modulation of F_0 in juvenile calls.

Computer simulation

Fig. 6 presents heat maps of the interacting effects of subglottal pressure, glottal gap and vocal fold tension on F_0. White regions correspond to aphonia (no tissue oscillation). Fig. 6A shows how F_0 depends on the glottal gap and tissue stiffness. Higher tension (facilitated by larger strain) was associated with higher F_0 sounds. As glottal gap was reduced, adduction increased and so did F_0. However, there seems to be a 'threshold tension' at 0.05, below which F_0 changes minimally with varying glottal gap. Only above this threshold does variation in adduction (at a given tension) have large effects on F_0.

Fig. 6B shows the influence of glottal gap size and subglottal pressure on F_0. It is well known that the subglottal pressure

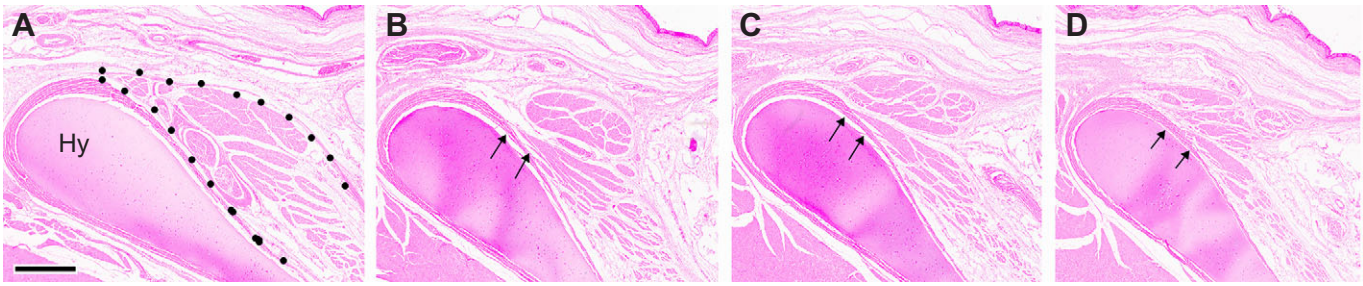

Fig. 4. Four serial cross-sections from a 2-year-old alligator of the caudal branch of musculus cricoarytenoideus, which attaches to the basihyoid cartilage. Distance between sections was 1 mm from rostral (A) to caudal (D). all sections are stained with H&E. The dotted line in A outlines the muscle attaching to the medial surface of the basihyoid (Hy). In B–D, muscle fibers approach and attach to the most dorso-lateral area of the basihyoid cartilage (indicated by arrows). This basihyoid attachment makes the cricoarytenoideus an extrinsic laryngeal muscle with consequences for laryngeal biomechanics. Scale bar: 500 μm.

The Journal of Experimental Biology (2015) 218, 991-998 doi:10.1242/jeb.117101

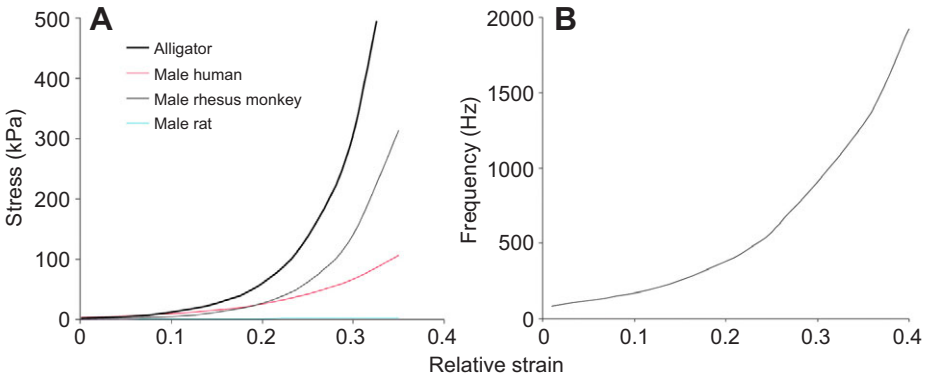

Fig. 5. Stress–strain relationship and fundamental frequency range for alligator vocal folds. (A) In tensile tests, connective tissue of vocal folds was repeatedly stretched by 40%. The loading phase was modeled with a linear and an exponential model. The average stress–strain relationship from six vocal folds is shown here. Comparative data from three mammals are also shown (human data from Chan et al., 2007; Rhesus monkey data from Riede, 2010; rat data from Riede et al., 2011). (B) Fundamental frequency range for a 1-cm-long alligator vocal fold derived with the string model (Eqn 4) implementing the average stress–strain relationship for an alligator vocal fold.

facilitates vocal fold vibration as long as a phonation threshold pressure (i.e. onset point of tissue vibrations) is exceeded. Dynamic stretch of the tissue during each vibration cycle is responsible for the dependence of F_0 on subglottal pressure. The borderline between aphonic and phonic regions corresponds to the phonation onset point, which decreases as adduction is increases (i.e. smaller glottal gap); in this way, pressure indirectly controls F_0. Subglottal pressure has an even more dramatic effect on increasing F_0 in the region where the glottal gap is very small – a phenomenon attributed to dynamic stretch and cubic nonlinearity of tissue properties.

Fig. 6C shows how both strain and subglottal pressure control F_0. The highest frequency of 930 Hz was achieved at a strain of 35% and subglottal pressure of 4 kPa. Subglottal pressure variations have maximal influence on F_0 when strain is large. At low strains, F_0 changes very little at a given pressure of 4 kPa.

Fig. 6D shows the time waveform, spectrogram and subglottal pressure pattern of a juvenile contact call (from Riede et al., 2011). F_0 starts at 900 Hz and is down-modulated to 100 Hz within 150 ms. The arrows in Fig. 6C indicate potential paths through the heat map that would produce this call. Note that multiple pathways are possible.

DISCUSSION

Alligator vocal folds have a complex morphology consisting of epithelium, lamina propria and muscle. The ECM of the lamina propria showed that collagen fibers are densely packed below the epithelium and less organized inside the vocal fold. The composition of the ECM is of central importance because of its crucial contributions to the mechanical properties of the vocal fold and the voice quality that results. Mechanical properties of the vibrating vocal folds set the boundaries for F_0. Tensile data suggest that small changes in length (up to 35% strain) of the rather stiff alligator vocal fold (compared with mammalian vocal folds) can facilitate F_0 values reported for juvenile alligator calls (50–1200 Hz). Complex, species-specific laryngeal morphologies (and associated sound-source properties) are widespread among mammals (e.g. Hirano, 1974; Riede, 2010; Riede et al., 2010; Frey and Riede, 2013; Klemuk et al., 2011) and have also been described for the labia, the avian analog of laryngeal vocal folds (Fee, 2002; Riede and Goller, 2014). In contrast to alligators, geckonid lizards (Moore et al., 1991; Rittenhouse et al., 1998; Russel et al., 2000) and tortoises (Sacchi et al., 2004) have higher numbers of elastic fibers in the subepithelial region of the vocal fold lamina propria. A purported vocal fold analog (‘fibrofatty laryngeal fold’: Fraher et al., 2010) has been described for leatherback sea turtles (*Dermodyles coriacea*). Thus, it is reasonable to expect species-specific morphologies in vocal folds/analogues as far back as basal reptiles.

Table 1. Parameters of linear (Eqn 1) and exponential (Eqn 2) models for curve-fitting the empirical stress–strain response of vocal fold and exponential decay model for curve-fitting the empirical stress relaxation curve

Parameter	Symbol	Value
Constant in Eqn 1	A	53±45
Constant in Eqn 1	B	−0.4±0.9
Constant in Eqn 2	a	2.4±2.9
Constant in Eqn 2	b	16.2±3.1
Linear strain limit	ε_1	10.9±3.4%
Hysteresis	H	38.5±7.8%
Peak stress	Y_0	745±260 kPa
Plateau stress	P	509±129 kPa
Rate constant	K	646±206 kPa s^{-1}
Half-life	HT	0.29±0.09 s
Relative energy loss	E	29.2±8.8%

An extrinsic laryngeal muscle

The cricoarytenoid muscle possesses a ventral portion connecting the cricoid and basihyoid cartilage. Because the attachment is extrinsic, contraction of this muscle moves the larynx relative to the basihyoid. Vocal fold tissue bridges the arytenoid cartilage (at the caudal portion of vocal fold) and basihyoid (at the cranial portion of vocal fold). The tissue would be strained along the cranio-caudal axis by contraction of the ventral branch of the cricoarytenoid muscle. Indeed, Henle (1839) ascribed a ‘larynx retractor’ function to this muscle (‘dilator glottidis’) in some reptiles, upon finding an extrinsic laryngeal insertion – a morphology not noted for alligators (Henle, 1839, Göppert, 1899; Göppert, 1937; Söller, 1931). It remains to be tested how this retractor function is employed during vocal production by alligators.

Previously, we assumed that alligator vocal folds are only stretched dynamically by means of oscillation. However, two additional mechanisms are possible. Dynamic stretch is a passive mechanism occurring during each vocal fold vibration and is below 5% in humans or in excised dog larynges (Titze, 1989). Muscle activation could also initiate longitudinal (cranio-caudal) elongation along the vocal-fold axis, but would require neural control. This establishes three variables under active control: lung pressure, longitudinal stiffness (regulated by the cricoarytenoid muscle) and adduction, affecting the glottal gap (regulated by the constrictor larynges muscle). The heat-map representation for three pairwise associations of these actively controlled variables demonstrates how F_0 regulation could be achieved. Determining the net effect of subglottal pressure, vocal fold length and adduction on F_0 is of great importance because it would indicate complexity of motor control comparable with that of vocalizing mammals.

The Journal of Experimental Biology (2015) 218, 991-998 doi:10.1242/jeb.117101

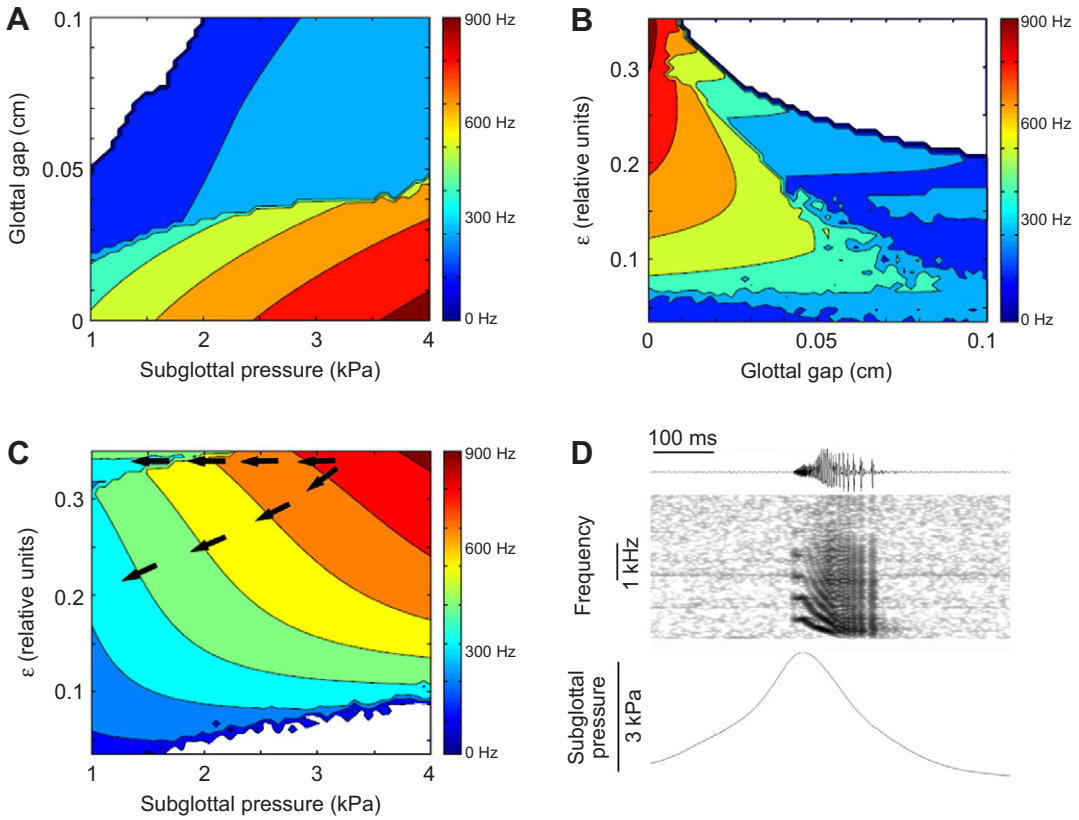

Fig. 6. Dependence of fundamental frequency (F_0) on glottal gap x_0, strain ε and subglottal pressure P_s. Color indicates F_0 in the range 0 Hz and 900 Hz. White color corresponds to an aphonic region. (A) The strain was fixed to ε=0.19, while the other parameters were changed as (P_s, x_0)∈[1,4]×[0,0.1]. (B) Subglottal pressure was fixed to P_s=2.5 kPa, while the other parameters were changed as (x_0, ε)∈[0,0.1]×[0,0.35]. (C) The glottal gap was fixed to x_0=0 cm, while the other parameters were changed as (P_s, ε)∈[1,4]×[0,0.35]. (D) Time waveform, spectrogram and subglottal pressure pattern of a juvenile contact call (from Riede et al., 2011). The arrows in C indicate potential pathways in parameter space to generate such a call.

The alligator larynx as myoelastic-aerodynamic sound source and its implications for sauropsid vocal production

This study and previous work (Riede et al., 2011) provide information on vocal production mechanisms in American alligators that may help illuminate broad evolutionary patterns. Most excitingly, the data suggest that alligators can employ complex motor control, and that basic design patterns described for the vocal folds of mammals and birds (Hirano, 1974; Riede and Goller, 2014) also apply to non-avian reptiles. Additional mechanical properties of cartilage framework and laryngeal muscles, as well as the possibility of active motor control remain to be explored. The potential for the downstream modulation (e.g. vocal tract filtering) seen in mammals and birds may exist, but this is unknown.

The data complement the picture of the alligator larynx as a myoelastic-aerodynamic sound source, a concept developed for human phonation (van den Berg, 1958; Titze, 2006) and applicable to the avian syrinx (e.g. Riede and Goller, 2010). Muscles actively position and stretch the oscillating tissue. Vocal sound output in alligators is therefore a result of the integration of active motor control of the larynx and the respiratory system, as well as the viscoelastic properties of the vocal folds. The airflow-induced (passive) oscillations of the vocal folds depend largely on the magnitude of the forces produced at the sound source. As in turtles, lizards, mammals and birds, alligator vocal folds are multilayered, suggesting convergent design that is functionally driven. Layered tissue confers anisotropic properties at the gross structural level, generating specific responses to different types of deformations (e.g. stretch and adduction). It follows that any change in lung pressure, vocal fold tension and/or adduction, will alter the effective stiffness of this multi-layered system – a parameter that changes how folds vibrate and thereby convert aerodynamic energy into acoustic energy. The computer simulation illustrates how these three variables dictate F_0. The simulation generates a large possible acoustic space, and suggests that multiple alternative variable combinations can generate the same acoustic output. Plotting an actual alligator call (Fig. 6) into the simulated acoustic space indicates that many of these variable combinations are biologically and physically possible.

The model considers three physiological variables (subglottal pressure, glottal adduction force and vocal fold tension). The exact measurements, however, exist only for subglottal pressure. The adduction force was therefore only estimated for the alligator larynx. The vocal fold abduction and adduction are nonetheless important, not only for swallowing and closure of the airway, but also for voice quality. In general, adduction first decreases the glottal gap to zero and then pushes the vocal folds against each other with increasing force. It is critical that the pre-phonatory positioning of vocal folds – the glottal gap – reduces the minimal subglottal pressure that is needed to sustain vocal folds oscillations (Titze, 1988). In humans, vocal fold posturing affects intensity and pitch of the voice (e.g. Murry et al., 1998; Honda, 1983), where adduction of the vocal folds is a key to optimize airflow–tissue interaction at voice onset (Titze et al., 1995; Chan and Titze, 2006). For the relatively low

The Journal of Experimental Biology (2015) 218, 991-998 doi:10.1242/jeb.117101

subglottal pressures measured in alligators (0.5 to 2 kPa at phonation onset) and for the given tissue properties, the assumption of a very small glottal gap seems justified. Variable adductive force had been suggested to play a role in control of fundamental frequency in alligators (Riede et al., 2011), but remains to be measured.

Finally, we also considered how sound production has evolved (Brazaitis and Watanabe, 2011) because of its implications for sexual selection and parental care. How the Permian and Triassic landscapes sounded and the mechanisms whereby non-avian dinosaurs and other extinct amniotes vocalized will remain speculative without a sufficient fossil record of vocal organs (e.g. Senter, 2008). The early steps will remain elusive if we only study the young stem groups. This study contributes to a critical phylogenetic bracket. Unifying control and design principles among the ancestral, derived and more distantly related groups (mammals) indicate functional constraints that may make it possible to discern vocal capabilities in extinct groups (e.g. Bass et al., 2008). This study contributes to these efforts because birds and crocodilians are sister taxa that bracket pterosaurs and non-avian dinosaurs, and thus these results shed some light on possible vocal fold morphology and function in the ancestral archosaur.

MATERIALS AND METHODS

Alligator (*Alligator mississippiensis* Daudin 1802) larynges were provided by the Alligator Tissue Bank at UC Irvine (courtesy of Tomasz Owerkowicz and Jim Hicks), by Ruth Elsey (Rockefeller Wildlife Refuge, Los Angeles, CA), by John V. Price (Insta-Gator, Ranch and Hatchery, Los Angeles, CA) and by the University of Utah Vertebrate Evolution lab.

Histology

Larynges of four females and two males were processed in order to investigate tissue composition of the vocal folds. The animals ranged in size between 0.05 kg (snout–vent length, SVL: 12 cm) and 12 kg (SVL: 81 cm). The tissue was fixed immediately after harvest in 10% neutral buffered formalin (SF100-4 Fisher Scientific) for 2 weeks and subsequently decalcified for 8 h (Surgipath Decalcifier 1), embedded in paraffin, and sectioned from rostral to caudal at 5 µm thickness at five subsequent levels which were 1 to 2 mm apart. Sections were exposed to hematoxylin and eosin (H&E) for general overview, elastica van Gieson stain (EVG) for elastin fibers, Masson's trichrome stain (TRI) for collagen fibers or Alcian Blue stain (AB) (pH 2.5) for mucopolysaccharides. We also performed a digestion procedure with bovine testicular hyaluronidase to test for relative HA compostion; if hyaluronan is a major component of the mucosubstances, incubation with hyaluronidase will destroy Alcian Blue positivity). Slides were first deparaffinized, then incubated in hyaluronidase at 37°C for 1 h, washed in running water for 5 min and finally stained with Alcian Blue. All stains were performed in conjunction with control stains (artery for EVG; liver for TRI; umbilical cord for AB). Images were digitized with a ScanScope CS2 scanner (Aperio, Vista, CA) and analyzed with Imagescope (Vista, CA) and ImageJ (NIH, open source).

Contrast enhanced micro-CT imaging

Computer tomographic (CT) imaging was used to investigate the morphology of soft and hard tissue components. Two specimens (1 male, 3 years, SVL: 45 cm; 1 male 7 years, SVL: 96 cm) were prepared at the Texas Natural History Collection (TNHC) and scanned at the University of Texas at Austin High-Resolution X-ray Computed Tomography Facility (UTCT). The tongue body with the intact larynx was fixed in 10% neutral-buffered formalin solution for 2 weeks and then transferred into ethanol (100%) to dehydrate for 8 days. The specimen was stained for 4 days in an iodine solution (I_2E, 1% w/v, after Metscher, 2009). Images were obtained at a resolution of 1024×1024 dpi and stored as 16-bit Tiff format files. The entire larynx region was investigated in 975 slices. Scan parameters were 180 kV, 0.32 mA, slice thickness 0.06969 mm, interslice spacing of 0.06969 mm and a field of reconstruction of 66 mm. CT images were imported into Avizo 6.3 (FEI Visualization Sciences Group) for segmentation of the laryngeal cartilages, muscular tissues and soft connective tissue. SurfaceGen was used to render the 3-D structures.

Tensile tests

Tensile tests were used to investigate stress response to longitudinal deformation. Vocal folds from four specimens (1 kg body mass, 1 cm vocal fold length, SVL: 33 cm) were studied. Connective tissue of a vocal fold was dissected by removing muscle tissue but keeping epithelium intact. The tissue was mounted vertically in a chamber containing Ringer's solution. The chamber was immersed in a water bath maintained at 38°C (see Riede, 2010, for an illustration of the testing apparatus). The length between fixation points was measured with a caliper (±0.1 mm accuracy). The tissue was pre-conditioned by straining it by 0.5 mm in three cycles at a rate of 1 Hz. Force and displacement data were obtained by 15 cycles of 1 Hz sinusoidal stretch-and-release with a dual-mode servo-control lever system (Aurora Scientific Model 305B, Aurora, ON, Canada; resolution 1 µm and 0.3 mN). Signals were recorded with a 16-bit analog-to-digital acquisition board (Windaq Model DI722, DATAQ Instruments; Akron, OH) at 3 kHz sampling frequency. After 2 min rest, stress relaxation was measured. The tissue was strained to 40% for 30 s.

The stress–strain relationship was modeled in two ways. The low-strain region was modeled with a linear function:

$$\sigma = A\varepsilon + B, \quad \text{for} \quad \varepsilon < \varepsilon_1, \tag{1}$$

where A is the slope of the curve, and B is the y-axis intercept. The high-strain region was approximated with an exponential equation:

$$\sigma = ae^{b\varepsilon}, \quad \text{for} \quad \varepsilon \geq \varepsilon_1, \tag{2}$$

where a and b are constants to be determined empirically, and ε_1 is the linear strain limit, which was derived by fitting a linear and exponential regression line, respectively, to the empirical data, while maximizing the sum of both regression coefficients. Hysteresis, i.e. the energy loss between loading phase and unloading phase, was estimated as the difference between the area under the curves of both phases.

The stress relaxation curve was modeled with an exponential 1-phase-decay function between maximum stress and 1 s thereafter:

$$\sigma(t) = (\sigma_0 - P) + e^{-Kt} + P, \tag{3}$$

where P is the estimated plateau, K are the rate constants for the fast and the slow relaxation, respectively, and σ_0 is the peak stress at time point zero (t_0). Half-life is computed as $\ln(2)/K$.

F_0 is an important acoustic feature. Understanding the causes of variation in F_0 is therefore paramount in understanding acoustic communication. Vocal fold viscoelastic properties are one important parameter determining F_0. At first approximation, the behavior of the vocal fold resembles that of a string fixed at each end. In alligators, the fixed points are the arytenoid cartilage (at one end) and the basihyoid cartilage (at the other end). The string model predicts that:

$$F_0 = \frac{1}{2L}\sqrt{\frac{\sigma}{\rho}}, \tag{4}$$

where L is the string (or vocal fold) length (measured along the rostro-caudal commissure), σ is the tissue stress at any given strain and ρ is the tissue density (1040 kg m^{-3}). Stress and strain data collected in the tensile tests were integrated in a two-mass computer model with a relaxed vocal fold length of 1 cm to simulate the vocalization of a juvenile alligator.

Computer simulation – two-mass model

A computational model of the alligator vocal folds had been constructed previously (Riede et al., 2011). Here, we employed this model to study how measurements of the elastic property and the dimension of the larynx contribute to the alligator call. Our interest was to clarify the dependence of F_0 on the three parameters: (1) vocal fold tension, which was measured in

The Journal of Experimental Biology (2015) 218, 991-998 doi:10.1242/jeb.117101

this study; (2) subglottal pressure, which ranges between 0.5 and 6 kPa (Riede et al., 2011); (3) vocal fold adduction. Alligators can alter the degree of glottal opening (i.e. adduction strength). Visual inspection in two vocalizing alligators (our unpublished data) suggested that vocal folds are adducted prior to vocalization. However, adduction strength has not yet been measured and was estimated in this study.

Anatomical investigations presented here indicate that alligators possess mechanisms (points 1 and 2 above) to control the tension of the vocal fold by modulating strain. Using the computational model, we studied F_0 ranges that can be produced and compared the computational outcome with previously recorded alligator vocalizations.

The two-mass model (Ishizaka and Flanagan, 1972; Steinecke and Herzel, 1995) describes the vocal fold tissue as a set of two masses coupled by springs (see Riede et al., 2011 for an illustration of the model). The phase shift of the two masses, representing, respectively, the upper and lower parts of the vocal fold, efficiently transfers the glottal flow energy to the vocal fold (Titze, 1988), generating vibrations.

The model equations are:

$$m_1\ddot{x}_{1\alpha}+r_1\dot{x}_{1\alpha}+k_1(x_{1\alpha}+\eta x_{1\alpha}^3)+\Theta(-a_1)c_1(a_1/2l)+k_c(x_{1\alpha}-x_{2\alpha})=ld_1P_1,$$
$$m_2\ddot{x}_{2\alpha}+r_2\dot{x}_{2\alpha}+k_2(x_{2\alpha}+\eta x_{2\alpha}^3)+\Theta(-a_2)c_2(a_2/2l)+k_c(x_{2\alpha}-x_{1\alpha})=ld_2P_2. \quad (5)$$

Here, m_1 and m_2 denote lower and upper masses, whereas $x_{1\alpha}$ and $x_{2\alpha}$ represent their respective displacements ($\alpha=l,r$ denotes either left or right side). k_i, and r_i are stiffness and damping of the lower and upper masses (i=1,2), where a cubic term is included to account for stiffness nonlinearity. k_c indicates mutual coupling between the two masses. Vocal fold length and the glottal gap are represented by l and x_0, giving lower and upper glottal areas of $a_i=l(x_0+x_{it}+x_{il})$. A negative glottal area means that the left and right masses are in collision, producing a repulsive force. During the glottal closure, the collision constant c_i is activated by a function defined as $\Theta(x)$=1 (x>0), 0 ($x\leq$0). For simplicity, symmetrical motion between the left and right vocal folds was assumed ($x_{1l}=x_{1r}$, $x_{2l}=x_{2r}$). The effect of the vocal tract acoustic loading was not considered.

Under the assumption that the flow inside the glottis obeys Bernoulli's Principle below the narrowest part of the glottis, the pressures that act on individual masses were calculated as $P_1=P_s\{1-\Theta(a_{min})(a_{min}/a_1)^2\}\Theta(a_1)$ and P_2=0, where P_s represents the subglottal pressure and $a_{min}=\min(a_1, a_2)$. The glottal flow was given as $U=(2P_s/\rho_{air})^{1/2}\ a_{min}\Theta(a_{min})$ using the air density constant (ρ_{air}=0.00113 g cm^{-2}).

The parameter values were set in accordance with our measurements. The length, width and depth of the vocal fold were set as l=1 cm, w=0.4 cm, and $d=d_1+d_2$=0.48 cm (d_1=0.4 cm, d_2=0.08 cm), respectively, corresponding to the vocal folds of a 1 kg alligator (45 cm snout–vent length). The masses were given by $m_1=\rho lwd_1$ and $m_2=\rho lwd_2$. Using the Young's modulus, which was estimated from the stress-strain curve as $E=\sigma'=abe^{b\varepsilon}$, the stiffness was computed as $k_1=wd_1E/l$, $k_2=wd_2E/l$. Following the standard setting, the nonlinear stiffness, the mutual coupling, and the collision constants were set as η=100, $k_c=k_1/3$, $c_1=3k_1$, $c_2=3k_2$. The damping constants were set as $r_i=2\zeta(m_ik_i)^{1/2}$ (i=1,2) using a damping ratio of ζ=0.05. Once the parameter values were fixed, Eqn 5 was integrated by the Euler method with a time step of Δt=1/3200 s. The glottal flow U was generated and analyzed by the FFT (Fast Fourier Transform) to compute F_0.

The main variables controlling phonation were strain ε (3 to 35%), subglottal pressure P_s (1 to 4 kPa), and glottal gap x_0. Strain determines vocal fold stiffness. A small glottal gap value represents a high level of adduction. Glottal gap was varied between 0 cm and 0.1 cm.

Acknowledgements
We are grateful for tissue donations from the Alligator Tissue Bank at UC Irvine (courtesy of Tomasz Owerkowicz and Jim Hicks; NSF grant IOS 0922756) and Ruth M. Elsey from the Rockefeller Wildlife Refuge, Louisiana Department of Wildlife and Fisheries, Grand Chenier, Louisiana.

Competing interests
The authors declare no competing or financial interests.

Author contributions
All authors conceived and designed the experiments; T.R., Z.L. and I.T.T. performed the experiments; T.R. and I.T.T. analysed the data; T.R. wrote the paper; all authors contributed substantially to discussion.

Funding
I.T.T. was supported by Grant-in-Aid for Scientific Research (No. 25540074, No. 23300071) from Japan Society for the Promotion of Science (JSPS). The work was also partially funded by NSF IOS - 1055080 to C.G.F.

Supplementary material
Supplementary material available online at
http://jeb.biologists.org/lookup/suppl/doi:10.1242/jeb.117101/-/DC1

References
Bass, A. H., Gilland, E. H. and Baker, R. (2008). Evolutionary origins for social vocalization in a vertebrate hindbrain-spinal compartment. *Science* **321**, 417-421.
Brazaitis, P. and Watanabe, M. E. (2011). Crocodilian behaviour: a window to dinosaur behaviour. *Historical Biol.* **23**, 73-90.
Britton, A. R. C. (2001). Review and classification of call types of juvenile crocodilians and factors affecting distress calls. In *Crocodilian Biology and Evolution* (ed. G.C. Grigg, F. Seebacher, C.E. Franklin), pp. 364-377. Chipping Norton, Australia: Surrey Beatty & Sons.
Campbell, H. W. (1973). Observations on the acoustic behavior of crocodilians. *Zoologica* **58**, 1-10.
Chan, R. W. and Titze, I. R. (2006). Dependence of phonation threshold pressure on vocal tract acoustics and vocal fold tissue mechanics. *J. Acoust. Soc. Am.* **119**, 2351-2362.
Chan, R. W., Fu, M., Young, L. and Tirunagari, N. (2007). Relative contributions of collagen and elastin to elasticity of the vocal fold under tension. *Ann. Biomed. Eng.* **35**, 1471-1483.
Fee, M. (2002). Measurement of the linear and nonlinear mechanical properties of the oscine syrinx: implications for function. *J. Comp. Physiol. A* **188**, 829-839.
Fraher, J., Davenport, J., Fitzgerald, E., McLaughlin, P., Doyle, T., Harman, L. and Cuffe, T. (2010). Opening and closing mechanisms of the leatherback sea turtle larynx: a crucial role for the tongue. *J. Exp. Biol.* **213**, 4137-4145.
Frey, R. and Riede, T. (2013). The anatomy of vocal divergence in North American elk and European red deer. *J. Morph.* **274**, 307-319.
Garrick, L. D. and Lang, J. W. (1977). Social signals and behavior of adult alligators and crocodiles. *Am. Zool.* **17**, 225-239.
Goller, F. and Riede, T. (2013). Integrative physiology of fundamental frequency control in birds. *J. Physiol.* **107**, 230-242.
Göppert, E. (1899). Der Kehlkopf der Amphibien und Reptilien. II. Theil. Reptilien. *Morph. Jahrb.* **28**, 1-27.
Göppert, E. (1937). Atmungssystem. I. Kehlkopf und Trachea. In *Handbuch der vergleichenden Anatomie der Wirbeltiere*, Vol. 3 (ed. L. Bolk, E. Göppert, E. Kallius and W. Lubosch), pp. 797-866. Berlin: Urban and Schwarzenberg.
Henle, F. G. J. (1839). *Vergleichend-anatomische Beschreibung des Kehlkopfes mit besonderer Berücksichtigung des Kehlkopfes der Reptilien*. Leipzig: Verlag von Leopold Voss.
Herzog, H. A. and Burghardt, G. M. (1977). Vocalizations in juvenile crocodilians. *Z. Tierpsychol.* **44**, 294-304.
Hirano, M. (1974). Morphological structure of the vocal cord as a vibrator and its variations. *Folia Phoniatrica* **26**, 89-94.
Honda, K. (1983). Variability analysis of laryngeal muscle activities. In *Vocal Fold Physiology: Biomechanics, Acoustics and Phonatory Control* (ed. I. Titze and R. Scherer), pp. 127-137. Denver, CO: The Denver Center for the Performing Arts.
Hunt, R. H. and Watanabe, M. E. (1982). Observations on maternal behavior of the American alligator, *Alligator mississippiensis*. *J. Herpetol.* **16**, 235-239.
Ishizaka, K. and Flanagan, J. L. (1972). Synthesis of voiced sounds from a two-mass model of the vocal cords. *Bell. Syst. Tech. J.* **51**, 1233-1268.
Klemuk, S. A., Riede, T., Walsh, E. J. and Titze, I. R. (2011). Adapted to Roar: Functional Morphology of Tiger and Lion Vocal Folds. *PLoS ONE* **6**, e27029.
Metscher, B. D. (2009). MicroCT for comparative morphology: simple staining methods allow high-contrast 3D imaging of diverse non-mineralized animal tissues. *BMC Physiol.* **9**, 11.
Moore, B. A., Russel, A. P. and Bauer, A. M. (1991). Structure of the larynx of the Tokay gecko (Gecko gecko), with particular reference to the vocal cords and glottal lips. *J. Morph.* **210**, 227-238.
Müller, J. (1839). *Compensation der physischen Kräfte am menschlichen Stimmorgan*, pp. 1-54. Berlin: Hirschwald Verlag.
Murry, T., Xu, J. J. and Woodson, G. E. (1998). Glottal configuration associated with fundamental frequency and vocal register. *J. Voice* **12**, 44-49.
Riede, T. (2010). Elasticity and stress relaxation of rhesus monkey (*Macaca mulatta*) vocal folds. *J. Exp. Biol.* **213**, 2924-2932.
Riede, T. and Goller, F. (2010). Peripheral mechanisms for vocal production in birds – Differences and similarities to human speech and singing. *Brain Lang.* **115**, 69-80.

Riede, T. and Goller, F. (2014). Morphological basis for the evolution of acoustic diversity in oscine songbirds. *Proc. R. Soc. B Bio. Sci.* **281**, 20132306.
Riede, T., Lingle, S., Hunter, E. J. and Titze, I. R. (2010). Cervids with different vocal behavior demonstrate different viscoelastic properties of their vocal folds. *J. Morph.* **27**, 1-11.
Riede, T., Tokuda, I. T. and Farmer, C. G. (2011). Subglottal pressure and fundamental frequency control in contact calls of juvenile *Alligator mississippiensis*. *J. Exp. Biol.* **214**, 3082-3095.
Rittenhouse, D. R., Russel, A. P. and Bauer, A. M. (1998). The larynx and trachea of the barking gecko, *Ptenopus garrulus maculatus* (Reptilia: Gekkonidae) and their relation to vocalization. *S. Afr. J. Zool.* **33**, 23-30.
Russel, A. P., Rittenhouse, D. R. and Bauer, A. M. (2000). Laryngotracheal morphology of Afro-Madagascan geckos: a comparative survey. *J. Morph.* **245**, 241-268.
Sacchi, R., Galeotti, P., Fasola, M. and Gerzeli, G. (2004). Larynx morphology and sound production in three species of testudinidae. *J. Morph.* **261**, 175-183.
Senter, P. (2008). Homology between and antiquity of stereotyped communicatory behaviors of crocodilians. *J. Herpetol.* **42**, 354-360.
Sicuro, F. L., Iack-Ximenes, I. E., Wogel, H. and Bilate, M. (2013). Vocal patterns of adult females and juveniles Caiman yacare. (Crocodilia: Alligatoridae) in Brazilian Pantanal wetland. *Rev. Biol. Trop.* **61**, 1401-1413.
Söller, L. (1931). Über den Aufbau und die Entwicklung des Kehlkopfes bei Krokodilen und Marsupialiern. *Morph. Jahrbuch* **68**, 541-593.
Steinecke, I. and Herzel, H. (1995). Bifurcations in an asymmetric vocal-fold model. *J. Acoust. Soc. Am.* **97**, 1874-1884.
Titze, I. R. (1988). The physics of small-amplitude oscillation of the vocal folds. *J. Acoust. Soc. Am.* **83**, 1536-1552.
Titze, I. R. (1989). On the relation between subglottal pressure and fundamental frequency in phonation. *J. Acoust. Soc. Am.* **85**, 901-906.
Titze, I. R. (2006). *The Myoelastic-Aerodynamic Theory of Phonation*. Salt Lake City, UT: National Center for Voice and Speech.
Titze, I. R., Schmidt, S. S. and Titze, M. R. (1995). Phonation threshold pressure in a physical model of the vocal fold mucosa. J. *Acoust. Soc. Am.* **97**, 3080-3084.
Todd, N. P. M. (2007). Estimated source intensity and active space of the American alligator (*Alligator mississippiensis*) vocal display. *J. Acoust. Soc. Am.* **122**, 2906-2915.
van den Berg, J. (1958). Myoelastic-aerodynamic theory of voice production. *J. Speech Lang. Hear. Res.* **1**, 227-244.
Vergne, A. L., Pritz, M. B. and Mathevon, N. (2009). Acoustic communication in crocodilians: from behaviour to brain. *Biol. Rev.* **84**, 391-411.
Vliet, K. A. (1989). Social displays of the American alligator (Alligator mississippiensis). *Am. Zool.* **29**, 1019-1031.
Wang, X., Wang, D., Wu, X., Wang, R. and Wang, C. (2007). Acoustic signals of Chinese alligators (*Alligator sinensis*): social communication. *J. Acoust. Soc. Am.* **121**, 2984-2989.
Wang, X., Wang, D., Zhang, S., Wang, C., Wang, R. and Wu, X. (2009). Why do Chinese alligators (*Alligator sinensis*) form bellowing choruses: A playback approach. *J. Acoust. Soc. Am.* **126**, 2082-2087.
Watanabe, M. E. (1980). The ethology of the American alligator with emphasis on vocalizations and response to vocalizations. PhD thesis, Biology Department, New York University, NY.

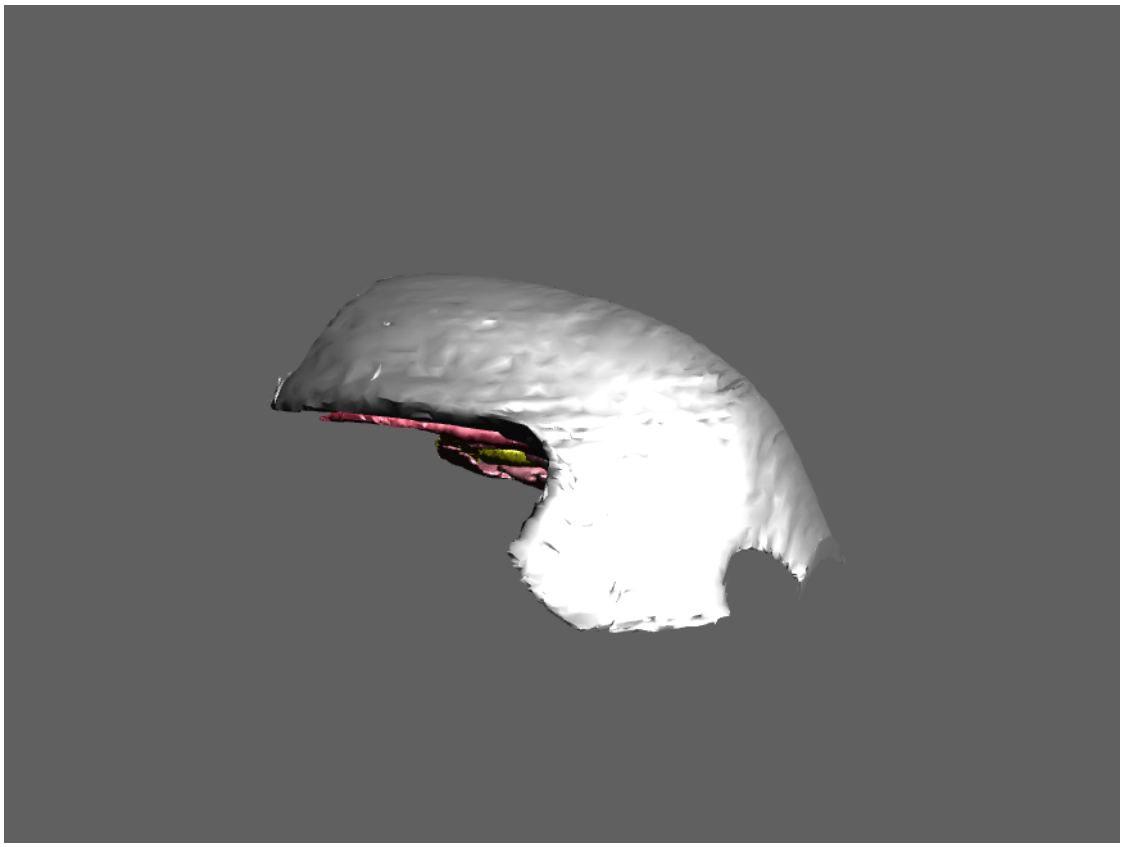

Fig. S1. Laryngeal cartilaginous framework and muscles of a male alligator larynx (interactive 3D PDF). This 3D PDF figure can be viewed with Adobe Acrobat Reader version 11 (http://www.adobe.com). Click on the figure to activate the 3D features. Use the 'toggle model tree' tool in Adobe Acrobat Reader to selectively show cartilages or soft tissue. This tool also provides labels for each structure.